

Femtosecond Dynamics of Molecules and Clusters

Abstract

The real-time dynamics of multiphoton ionization and fragmentation of molecules — Na_2 , Na_3 — and clusters — Na_n , Hg_n — has been studied in molecular beam experiments employing ion and electron spectroscopy together with femtosecond pump-probe techniques. Experiments with Na_2 and Na_3 reveal unexpected features of the dynamics of the absorption of several photons as seen in the one- and three dimensional vibrational wave packet motion in different potential surfaces and in high laser fields. Cluster size dependent studies of physical properties such as absorption resonances, lifetimes and decay channels have been performed using tunable femtosecond light pulses in resonance enhanced multiphoton ionization (REMPI) of the cluster size under investigation. This method failed in ns-laser experiments due to the ultrafast decay of the studied cluster. For Na_n cluster we find that for cluster sizes $n \leq 21$ molecular excitations and properties prevail over collective excitations of plasmon-like resonances. In the case of Hg_n cluster prompt formation of singly and doubly charged cluster are observed up to $n \approx 60$. The transient multiphoton ionization spectra show a ‘short’ time wave packet dynamics, which is identical for singly and doubly charged mercury clusters while the ‘long’ time fragmentation dynamics is different.

Introduction

Multiphoton ionization of small molecules has been studied in recent years by a variety of techniques and is generally well understood. The ionization is predominantly due to resonance-enhanced multi-photon (REMPI) processes, whereas nonresonant multiphoton processes only play a minor role. Dynamical aspects of the interaction of laser radiation with molecules and details of the excitation processes and the different decay channels of highly excited states, embedded in the ionization and in the fragmentation continuum, are rarely studied up to now. Recently we reported on the interaction of a bound doubly excited molecular state with different continua and the competition between the various decay channels (1). In that study we used femtosecond laser pulses as an

experimental tool to distinguish between the dissociative ionization of the molecule and the neutral fragmentation with subsequent excited-fragment photoionization. Both processes are difficult to distinguish when using nanosecond or even picosecond laser pulses. This distinction is of particular importance in multiphoton ionization studies of metal cluster systems. The multiphoton ionization and fragmentation of alkali metal molecules and, in particular, of Na_2 and Na_3 has attracted considerable current interest. In many experiments with Na_2 it has been found that, in conjunction with the formation of Na_2^+ ions, ionic fragments Na^+ are also formed. Resonance-enhanced multiphoton ionization (REMPI) processes via the $A\ ^1\Sigma_u^+$ or the $B\ ^1\Pi_u$ states are responsible for this observation (2). The sodium trimer Na_3 is probably the most studied and best known small metal-cluster (3). Its excitation spectrum consists of several bands due to different excited electronic states among which the B-state with an onset at 625 nm is of greatest interest. This is because of the observed pseudorotational features in the spectra. In a series of beautiful experiments Zewail and coworkers (4) have demonstrated the enormous advantage of applying femtosecond lasers to the study of molecular dynamics. Their pioneering work in the field of femtosecond photochemistry and transient molecular fluorescence spectroscopy has initiated other time-resolved ultrafast laser studies (5).

In recent years cluster and in particular metal cluster have been the fascinating subject of many experimental and theoretical studies. Cluster form the link between surface chemistry and molecular physics. Metal cluster exhibit distinct features ranging from molecular properties seen in small particles to solid state-like behaviour of larger aggregates. Studies of cluster properties like geometric structures, the evolution of the electronic states from localized to delocalized in nature and the real-time dynamics of ionization and fragmentation have yet not been studied in detail as a function of cluster size. In this contribution we report the first experiments in cluster physics employing ultrashort laser pulses to time-resolved studies of cluster ionization and fragmentation processes. Alkali cluster, which are easily formed in supersonic expansions, are attractive species to be studied experimentally and theoretically, because there is only one valence electron per atom.

Time-resolved measurements often open up new directions and provide a more comprehensive view of the physical and chemical processes. Due to recent developments in the generation and amplification of ultra-short light pulses, direct measurements of transient ionization and fragmentation spectra with femtosecond time resolution are now possible. This allows a closer look at the dynamical aspects of multiphoton ionization and fragmentation of molecules and clusters.

In this paper we discuss experimental results of time-resolved studies of multiphoton ionization and fragmentation processes of sodium and mercury molecules and cluster in molecular/cluster beam experiments applying femtosecond pump-probe techniques and ion and electron spectroscopy.

Experiment

In our femtosecond laser-molecular/cluster beam studies of time-resolved multi-photon ionization and fragmentation processes, we employed a combination of different experimental techniques. Femtosecond pump-probe techniques are used to induce and to probe cluster transitions, to resolve the interactions and to display the evolution of coherences and populations in real-time. A seeded supersonic beam provides the molecules and cluster in a collision-free environment and restricts the initial states to the very lowest vibrational and rotational states. Time-of-Flight (TOF) spectroscopy is used to measure the final continuum states, the cluster-size distributions and to determine the released kinetic energy of the ionic fragments and the energy distribution of the ejected electrons. Fig. 1 shows the schematic experimental arrangement of the cluster beam, the femtosecond laser pulses and the ion and electron TOF-spectrometers. The sodium cluster Na_n are produced by coexpansion of sodium vapor (50-100 mbar) with the inert carrier gas argon (1-8 bar) through a small cylindrical nozzle of about $100 \mu\text{m}$ diameter. This technique provides efficiently cooled sodium cluster with about 30-50 K vibrational temperatures. For mercury cluster Hg_n , the necessary oven temperatures are much lower. Femtosecond light pulses are generated in

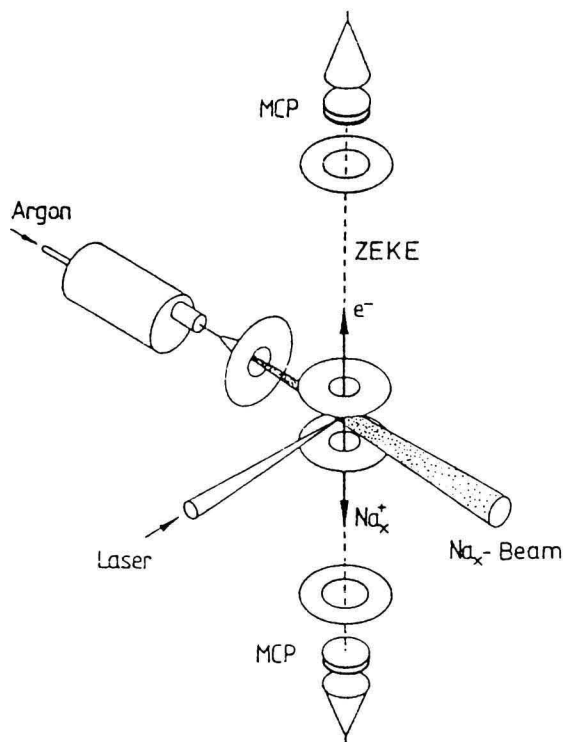


Fig. 1. Schematic experimental arrangement.

two different home-built laser systems. Tunable femtosecond pulses of 50 fs-100 fs time duration and of 0.1 μJ -50 μJ energy in the wavelength range 420 nm to 750 nm are generated in the laser system shown in Fig. 2. The output pulses of a colliding-pulse mode-locked ring dye laser (CPM) are amplified in a bow-tie amplifier, which is pumped by an excimer laser at 308 nm, pulse compressed and focussed into a cell containing methanol to generate a white light continuum. Light pulses at specific wavelengths selected from the white light continuum.

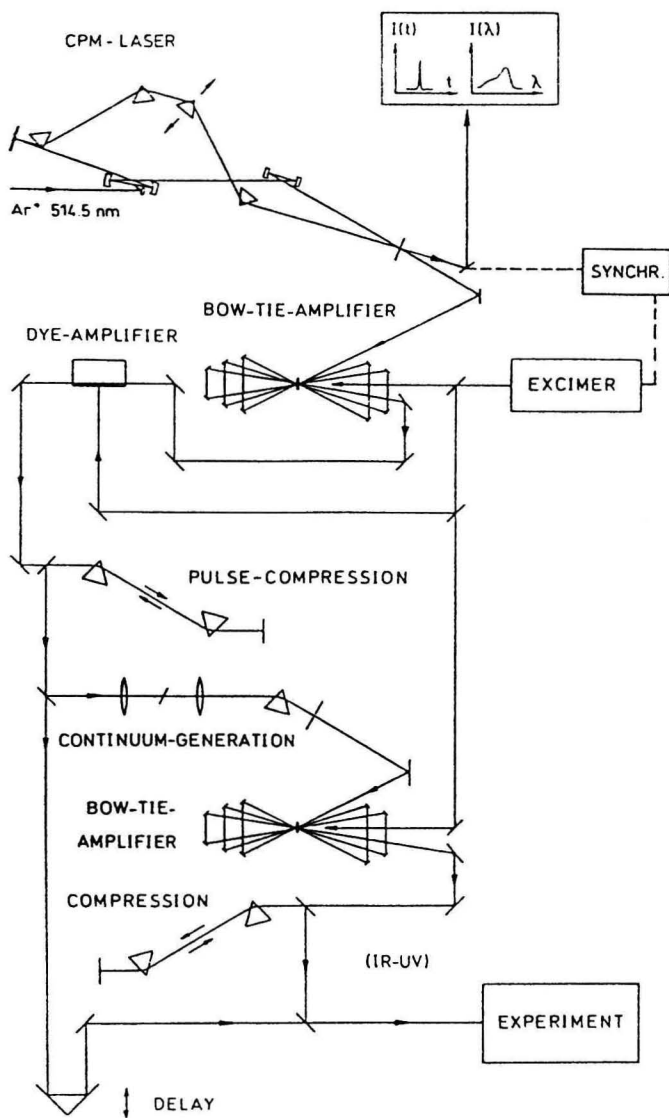


Fig. 2. Femtosecond laser system.

tinuum are amplified again in another bow-tie and compressed before entering the interaction region. A Michelson arrangement was used to delay the probe laser relative to the pump laser.

The second femtosecond laser system makes use of a home-built Ti : Sapphire laser oscillator. This Ti : Sapphire laser produces light pulses of 20 fs-70 fs time duration in the wavelength range 700 nm to 850 nm. Using again a bow-tie amplifier, pulse energies sufficient for multiphoton ionization of metal clusters are obtained.

Results and Discussion

Na_2 -Dimer

We have recently reported femtosecond time-resolved multiphoton ionization and fragmentation dynamics of the Na_2 molecule. From the real-time observation of vibrational wave packet motions it was concluded, that two different physical processes determine the time evolution of multiphoton ionization (6). The observed femtosecond pump-probe delay spectrum of the molecular ion (Na_2^+) signal is shown in Fig. 3. Evident from the beat structure seen in Fig. 3, there are two frequencies involved and therefore there are two contributions to the transient ionization spectrum, and the envelope intensity variation reveals them to be 180° out of phase. A Fourier analysis of this spectrum yields two groups of frequencies, one centered at 108.7 cm^{-1} and a second one centered at 92.0 cm^{-1} . From the observed two oscillation periods, the 180° phase shift and the additionally measured time-resolved Na^+ photofragmentation spectrum (7),

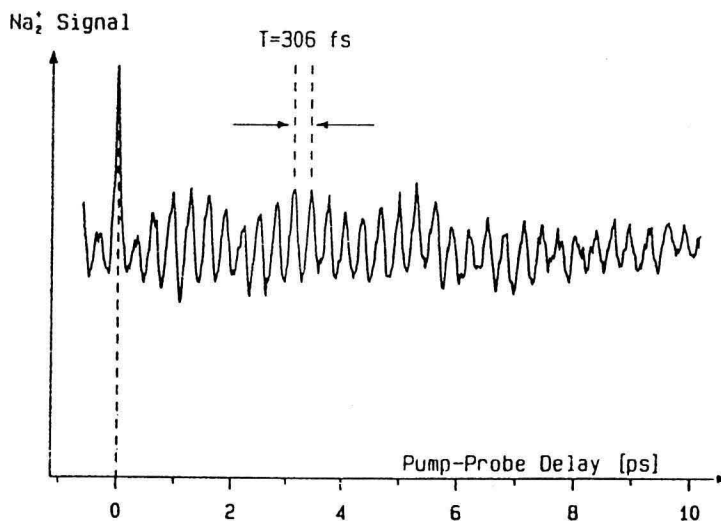


Fig. 3. Transient multiphoton-ionization spectrum of Na_2 .

we concluded that for Na_2 two different multiphoton ionization processes exist, to require incoherent addition of the intensities to account for the observations. The direct photoionization of an excited electron, where one pump photon creates a vibrational wave packet in the $A \ ^1\Sigma_u^+$ state and two probe photons transfer that motion via the $2 \ ^1\Pi_g$ state into the ionization continuum, is one (REMPI) process. The second involves excitation of two electrons and subsequent electronic autoionization. Here two pump photons create a wave packet at the inner turning point, in the $2 \ ^1\Pi_g$ Rydberg state, which then propagates to the outer turning point, where the probe laser transfers the motion into the continuum by exciting a second electron, forming a doubly excited neutral $\text{Na}_2^{*}(nl, n'l')$ molecule. This happens only at the outer turning point of the $2 \ ^1\Pi_g$ state periodically after each round trip. In this case the probe photon is absorbed at the earliest about 180 fs after the pump photons were absorbed. In the one electron direct photoionization process all three photons are absorbed at the inner turning point at once or at least within the time duration of the light

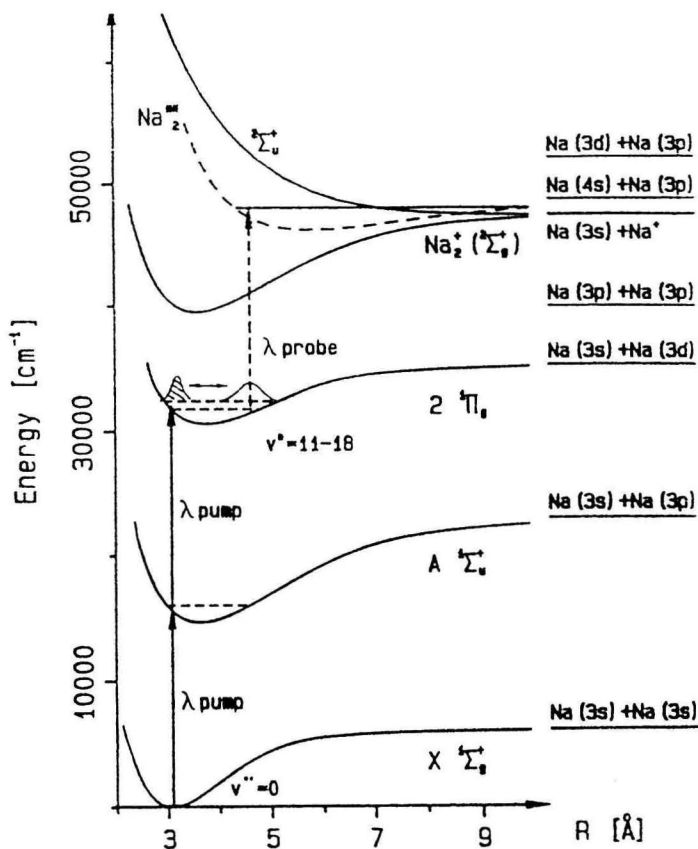


Fig. 4. Potential curve diagram illustrating the preparation of the wave packet in the $2 \ ^1\Pi_g$ state.

pulses. Figure 4 illustrates the two-photon-pump and one-photon-probe ionization process which involves excitation and decay of doubly excited states.

The Na_2 case is the first example of a femtosecond molecular multiphoton ionization study. It was only through time domain measurements that the existence of a second major ionization process was established. A comprehensive discussion including a comparison between experiment and quantum mechanical calculations can be found in a recent publication (8). In a further study the dependence of the total Na_2^+ ion signal on the intensity of the femtosecond pulses was investigated in detail (9). For higher laser intensities the relative contribution from the $A\ ^1\Sigma_u^+$ and the $2\ ^1\Pi_g$ states change dramatically, indicating the increasing importance of the two-electron versus the one-electron process. For even stronger fields ($10^{12}\ \text{W}/\text{cm}^2$) a vibrational wave packet in the electronic ground state $X\ ^1\Sigma_g^+$ is formed through stimulated emission during the time the ultrashort pump pulse interacts with the molecule, and its dynamics is also seen in the transient Na_2^+ signal. The spreading and recurrence of the vibrational wave packet in the bound $A\ ^1\Sigma_u^+$ electronic state has been studied in pump-probe experiments and compared with time-dependent quantum calculations (10).

Na_3 -Trimer

The same experimental set up and techniques have now been employed to study the ionization and fragmentation dynamics of the cluster Na_3 (11). In all the pump-probe experiments discussed here the same color has been used for the pump and the probe laser. This has the experimental advantage of a precise zero delay time determination and it facilitates the interpretation of weak structures superimposed on some decay curves. In the case of the B-state an ultrashort 60 fs pump pulse with photons of 623 nm excites a coherent superposition of the lowest vibrational and pseudorotational levels due to its bandwidth of about $300\ \text{cm}^{-1}$. The generated vibrational and pseudorotational wave packets propagate in the excited state potential surfaces. A time delayed probe photon of the same wavelength and the same 60 fs time duration probes the motion of the wave packet and the decay of the excited state population. This is done by time delayed probe photon ionization. The transient ionization spectrum of Na_3 obtained for a central wavelength of 623 nm is shown in Fig. 5. This time domain spectrum is more complex than that observed for the dimer Na_2 . But still there are distinct recognizable time patterns, like the 320 fs separation of the major peaks, which corresponds to an energy of $105\ \text{cm}^{-1}$, and the dip around zero time delay caused by fragmentation of the formed Na_3^+ by the intense laser fields at $\Delta t = 0$. It is in agreement with earlier high resolution two photon ionization (via B-state) spectra (12) that we do not observe a decay of the B-state for delay times up to 10 ps. As the Fast Fourier Transformation (FFT) spectrum, displayed in Fig. 6, shows, the dynamics of the two photon ionization process is determined by three dimensional wave packet motions in the Na_3 B-state and in the X-state as well. At the applied laser intensity both states are involved. The

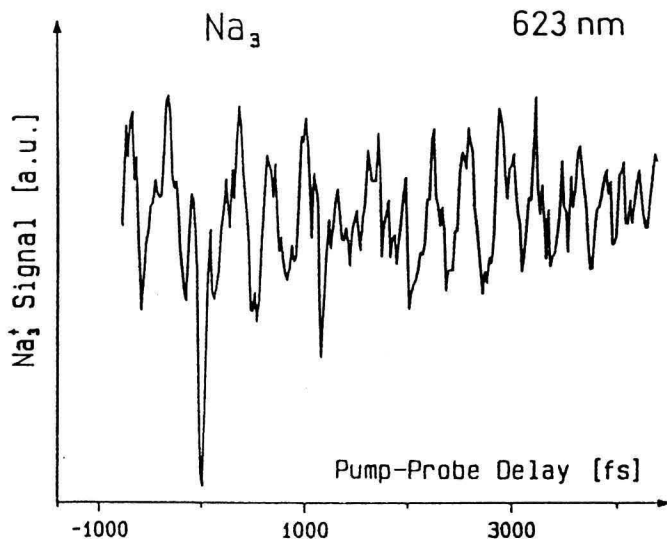


Fig. 5. Pump-probe ionization spectrum of Na_3 (B) using 60 fs light pulses at 623 nm.

pump laser generates a wave packet in the intermediate B-state and simultaneously a wave packet in the \bar{X} electronic ground state through stimulated emission pumping during the pump pulse. The contributions in the FFT spectrum (Fig. 6) near 140 cm^{-1} , 90 cm^{-1} and 50 cm^{-1} are attributed to the symmetric stretch, to the asymmetric stretch and to the bending mode in the Na_3 electronic ground state. This assignment is based upon the analysis of Broyer et al. (13). The wave packet dynamics in the excited B-state seems to be dominated by the symmetric stretch mode with frequencies close to 105 cm^{-1} . According to calculations of Meyer et al. (14) and Cocchini et al. (15), the Eigenfrequencies

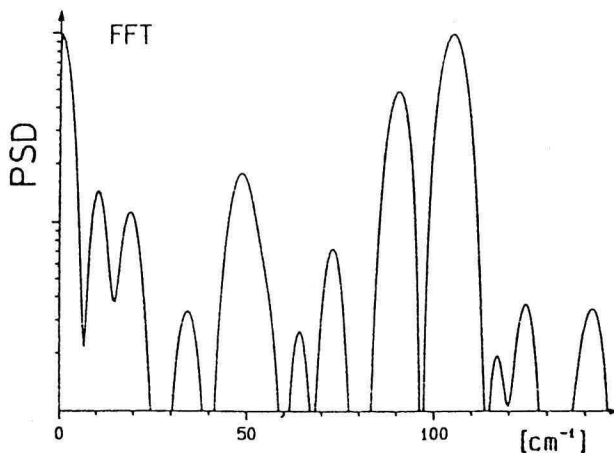


Fig. 6. Fourier (FFT) spectrum of Na_3 (B) transient ionization spectrum shown in Fig. 5.

of the symmetric stretch modes of the $4\ ^2A_1$ and the $3\ ^2B_2$ -states are in the range of 94 cm^{-1} to 111 cm^{-1} . The contribution around 72 cm^{-1} is tentatively assigned to the bending and asymmetric stretch mode of the $3\ ^2B_2$ state.

The other observed frequencies $8.5\text{-}12\text{ cm}^{-1}$, $17.5\text{-}20\text{ cm}^{-1}$ and $30.5\text{-}35\text{ cm}^{-1}$ are assigned to a free pseudorotational wave packet motion in the potential surface of the B-state. The energy differences of successive pseudorotational j -states are experimentally determined as assigned by Delacretaz et al. (12) on the basis of a pure Jahn-Teller distortion of the B-state to half-integer j -values. For $v=0$, ($v=1$), these values are $\Delta_j: 1/2, -3/2 = 2.5; (5)\text{ cm}^{-1}$, $\Delta_j: -3/2, 3/2 = 12; (13.5)\text{ cm}^{-1}$, $\Delta_j: 3/2, 5/2 = 18; (20)\text{ cm}^{-1}$, $\Delta_j: 7/2, 9/2 = 34; (30)\text{ cm}^{-1}$, respectively. It is however very interesting to note, that in our experiment the corresponding radial component (128 cm^{-1}) of the pseudorotational motion plays only a minor role, if at all. In contrast to this, high resolution spectroscopy of the B-X system exhibits a strong contribution of the radial pseudo-rotational component (12). Theoretical studies of Meiswinkel and Köppel (16) showed, that the observed high resolution spectra can also be explained taking into account a Pseudo-Jahn-Teller (PJT) model with integer pseudorotational j -values. In that model the vibronic coupling of the accidentally degenerate (D_{3h})-states $3\ ^2E'$ (B) and $2\ ^2A'_1$ is responsible for the observed vibronic structure. So far, it is not yet clear, which of the two models is more appropriate to explain the observed pseudorotational wave packet motion, since the ultrashort dynamics depend on the pseudorotational energy *differences*.

Na_n -Cluster

Recently we reported the first femtosecond time-resolved experiments in cluster physics (17), where the photofragmentation dynamics of small sodium cluster ions Na_n^+ have been studied with pump-probe techniques. Ultrashort laser pulses of 60 fs duration are employed to photoionize the sodium cluster and to probe the neutral photofragments. We find that the ejection of dimer Na_2 and trimer Na_3 photofragments occur on ultrashort time scales of 2.5 ps and 0.4 ps, respectively. This and the absence of cluster heating reveals that direct photo-induced fragmentation processes are important at short times rather than the statistical unimolecular decay.

Femtosecond laser pulses have been applied by our group to study cluster size-dependent properties like energy, bandwidth and lifetime(s) of intermediate resonances (Na_n^*) in beam experiments (18). Since the complexity of the spectroscopy and dynamics of metal cluster strongly increases with the number of atoms we have restricted our studies in the case of sodium cluster to sizes $n \leq 21$, whereas for mercury cluster we followed the size dependent properties up to $n \approx 45$.

The photoabsorption spectra of neutral metal cluster are of particular interest in view of the size-dependent transition from molecule-like absorption to collective excitation of the valence electrons. For larger cluster Na_n with $n \geq 4$, these

resonances are yet not observed in two photon ionization spectroscopy employing nanosecond or picosecond laser pulses because of the anticipated fast decay of the intermediate Na_n^* states. However, using nanosecond laser depletion spectroscopy, Knight (19) and Kappes (20) measured these spectra for selected cluster sizes. We have measured the energy and the bandwidth of Na_n^* ($n = 4-21$) metal cluster absorption resonances by femtosecond two-photon ionization spectroscopy in the range 1.5 eV-3.0 eV with tunable laser pulses. The most striking results, which are discussed in this contribution, are obtained for the cluster Na_8 and Na_{20} . Within the shell model (21) for the electronic structure of metal cluster, these cluster-sizes have a closed electronic shell and are therefore spherically symmetric. On the basis of the Jellium model, the Mie-Drude theory predicts for this spherically symmetric metallic cluster a single intense band corresponding to a classical surface-plasma oscillation. In more elaborate calculations based on (RPA) random-phase-approximations (22) or (TDLDA) time-dependent local-density-approximations (23) the photoabsorption strength, of for instance Na_{20} , splits into two strong and several weaker peaks. However, the fs-two photon ionization spectra of Na_8 - displayed in Fig. 7 - and Na_{20} - displayed in Fig. 8 show several strong resonances, in better agreement with ab initio molecular type calculations (24), with different bandwidths and as discussed later different lifetimes (25). This indicates that the simple physical picture based on the Jellium model has to be modified in order to explain these data.

No measurements of the intermediate resonance lifetime(s) have been reported so far. In our first experiments we have employed femtosecond pump-probe spectroscopy with tunable fs-laser pulses to measure the decay time(s) of the different absorption resonances of all Na_n cluster-sizes up to $n \leq 21$. In particular, the results obtained for Na_8 and Na_{20} are discussed in the following. Three transient ionization spectra of Na_8 , each obtained with the fs-laser tuned to the

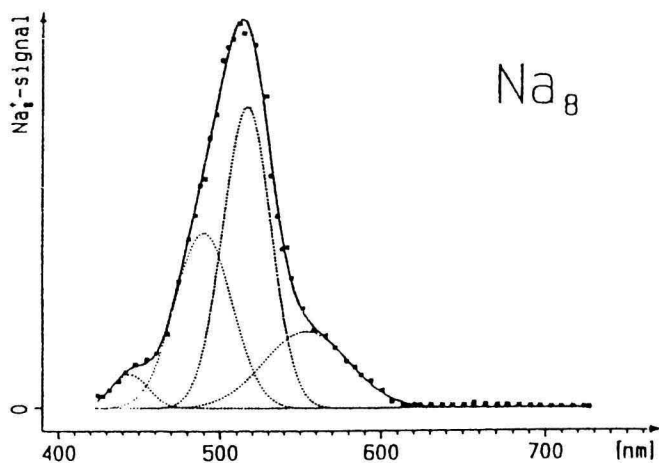


Fig. 7. Femtosecond two-photon ionization spectrum of Na_8 .

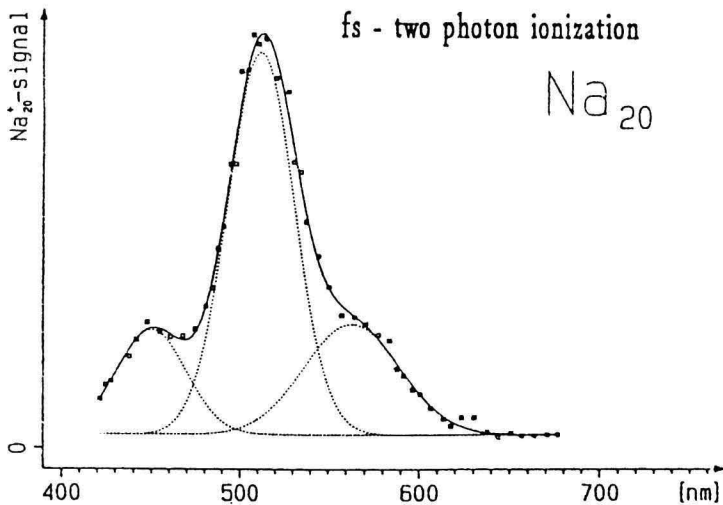


Fig. 8. Femtosecond two-photon ionization spectrum of Na_{20} .

center wavelength of the individual resonance, are displayed in Fig. 9. A pump pulse of about 80 fs time duration excites the Na_8 cluster while a time delayed identical probe pulse probes the residual population by photoionizing Na_8^* , the intermediate excited electronic states. As already discussed we have applied this technique to Na_2 , Na_3 and Na_n^+ to investigate wavepacket motion and fragmentation dynamics of these systems. Figure 9 shows the transient Na_8^+ spectra at 493 nm, 518 nm and 540 nm, where the Na_8^+ signal is plotted versus the pump-probe delay time. These spectra are symmetric with respect to zero delay time, because pump and probe pulses have the same time duration and intensity. In order to get the decay time constants we have fitted the transient spectra with a sum of exponential decay functions. At 518 nm the best fit is achieved by taking into account two functions with time constants of 0.5 ps and of about 4 ps. The transient spectrum at 493 nm shows only a single exponential decay with a time constant of 0.45 ps. What is however clearly demonstrated by the spectra in Fig. 9 is that each resonance has its own decay dynamics. Besides the decay there is also for each resonance an additional superimposed oscillatory structure. For the 518 nm resonance we find a regular oscillation with a time interval of about 160 fs, while at 493 nm there are at least two different series with time intervals of 360 fs and 270 fs. The transient spectrum of the 540 nm resonance is quite different from the others. Here we observe a much slower dynamics with time constants of 0.8 ps and of 2.8 ps. A Fast Fourier Transformation (FFT) of each of the time domain spectra clearly shows the corresponding frequencies and some additional frequencies in the range 30 cm^{-1} to 150 cm^{-1} . All these frequencies are in the range of the known vibrational Eigenfrequencies of Na_3 and Na_4 as determined by ZEKE-photo-electron spectroscopy (26). Thus, we believe the observed superimposed fast oscillations are due to wave packet motions in the potential surfaces of these metal-cluster. With the fs-laser tuned to 511 nm,

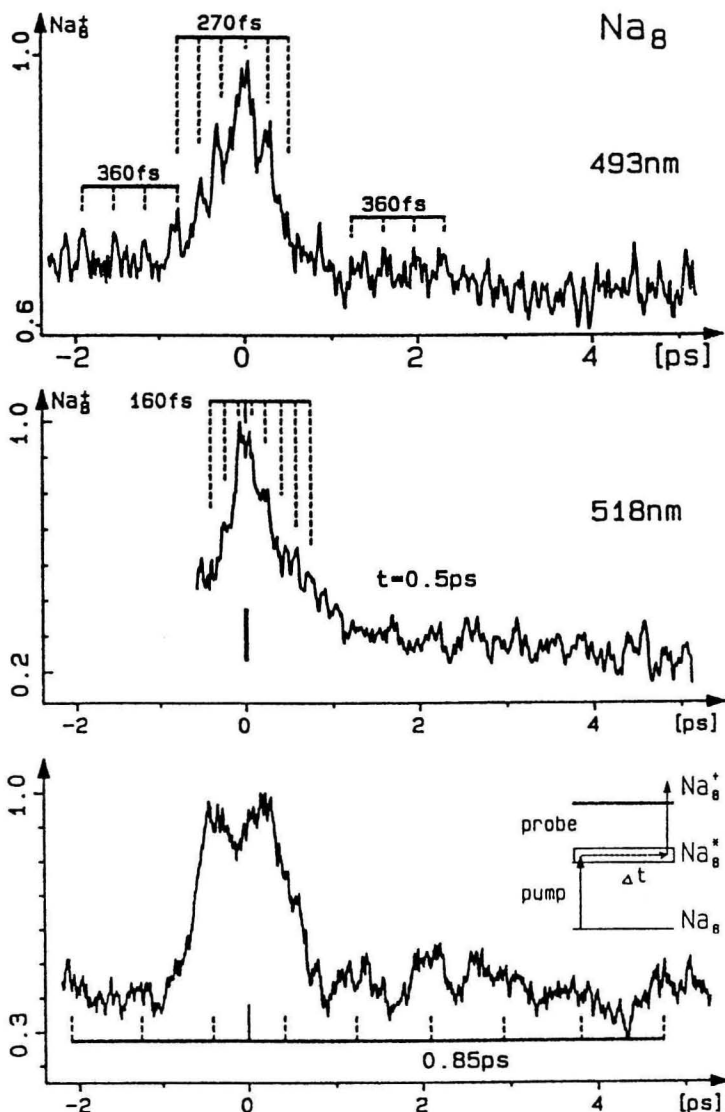


Fig. 9. Femtosecond time-resolved decay of the Na_8^* resonance at 493 nm, 518 nm and 540 nm measured with 80 fs pump and probe pulses.

the wavelength of the strongest resonance measured for Na_{20} , we observed a pump-probe spectrum which can be fitted by a single exponential decay with a time constant of 0.9 ps. Again there is an oscillatory structure superimposed with a time period of 360 fs. Note that also for Na_{20} , the decay time constant as well as the superimposed faster dynamics depend on the particular resonance. From these measurements with ultrafast laser pulses it is evident that the simple picture of a homogeneously broadened surface plasmon resonance is clearly not

appropriate to describe the optical excitations of small ($n \leq 21$) sodium metal-cluster. Furthermore the wavelength dependence of the decay time constants and the superimposed fast dynamics is in much better agreement with the measured structure of the cluster absorption resonances. As for the cluster resonances, the pump-probe measurements are much better understood taking into account molecular structures and excitations rather than considering the small Na_n cluster to be a metal with excitations of delocalized electrons. On the basis of the observed cluster absorption resonances, their ultrashort lifetimes and different decay patterns, we conclude that at least for cluster sizes Na_n with $n \leq 21$, molecular excitations and properties prevail over collective excitations and surface-plasmon like properties.

Hg_n -Cluster

Cluster form a new class of materials, which often exhibit unexpected properties. A very interesting situation arises with mercury cluster. The mercury atom has a $5d^{10} 6s^2 np^0$ closed shell electronic configuration with an ionization potential of 10.4 eV. Diatomic Hg_2 and other small mercury cluster are predominantly van der Waals bound systems. However, the electronic structure changes strongly with increasing cluster size and finally converges towards the bulk, where the 6s- and 6p bands overlap, giving mercury its metallic properties. This means that for the divalent Hg_n -cluster a size dependent transition from van der Waals to covalent to metallic binding exists. Therefore mercury provides the

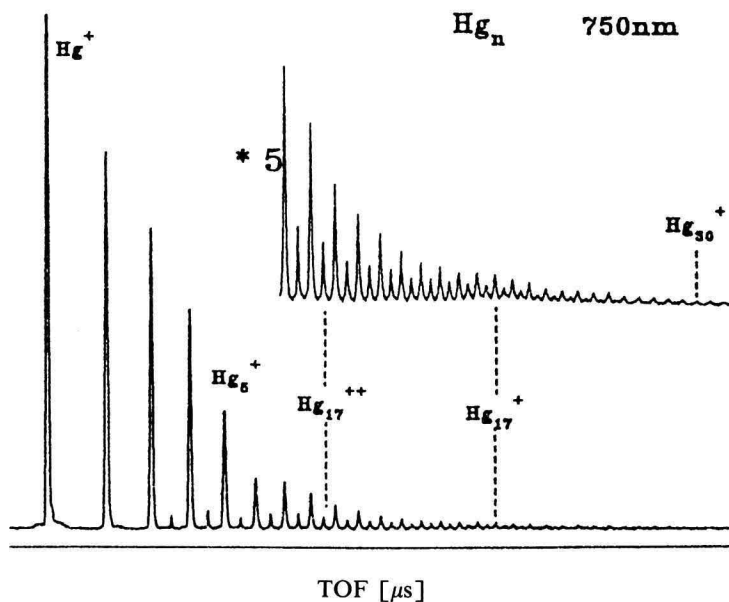


Fig. 10. Time-of-Flight mass spectrum of singly and doubly charged mercury cluster.

ideal system to study the size-dependent nonmetal-metal transition. For neutral mercury cluster the ionization potentials are reasonably well known (27), but other optical properties are practically unknown. The situation is much better for singly and doubly ionized Hg_n cluster with the recently reported ionization potentials and optical absorption spectra (28).

Here we report studies of multiphoton ionization and fragmentation of mercury cluster in the femtosecond time domain. We observe the prompt formation of singly and doubly charged cluster ions, and measure directly the decay of parent ions due to photofragmentation, together with the subsequent growth of daughter species. Furthermore we observe size-selected ion intensity oscillations in pump-probe measurements indicating wave packet dynamics in both singly and doubly charged cluster. For these experiments we have used a Ti:Sapphire laser generating a train of light pulses of 20 fs-70 fs time duration. The pulses are amplified, compressed and delayed to form a sequence of pump-probe pairs. Time-of-Flight (TOF) spectroscopy determines the mass of the cluster ion and the initial kinetic energy of the ionic fragments.

Figure 10 shows a TOF mass spectrum of singly and doubly charged Hg_n cluster ions produced by 30 fs pulses at 750 nm. The most striking features of the spectrum are first, that a multiphoton (6/12 photons) absorption forms singly and doubly ionized cluster and second, that the intensity ratio between singly and doubly charged cluster of the same mass is in most cases favour of the doubly charged species. Furthermore this ratio does not change for up to ten times lower laser intensity, but the ratio does change strongly with wavelength. For Hg_{17} clusters the ratio Hg_{17}^{++} to Hg_{17}^+ varies from 5:1 for 750 nm to 1:2 for 620 nm laser radiation. The lower part of Fig. 11 shows the transient ionization signal for the mercury dimer for short delay times while the upper part shows the evolution of the transient signal up to 160 ps delay. The oscillating signal at short delay times is due to a very strongly damped vibrational wave packet motion in an unknown excited electronic state of the mercury dimer. A Fourier analysis yields about 30 cm^{-1} , which is close to vibrational Eigenfrequencies of the van der Waals bound Hg_2 molecule. At longer delay times the figure shows first a 6 ps recovery and then a 20 ps decay of the total Hg_2^+ signal. It is inferred from the fragmentation kinetics of larger cluster, that Hg_{15}^+ fragments with a decay constant of 6 ps. Although nothing definitive can be stated without thorough analysis of all possible decay channels, the data suggest that at least one of the Hg_{15}^+ fragments is the dimer Hg_2 .

A very surprising result of our time-resolved studies of size-selected neutral mercury cluster is shown in Fig. 12. The figures detail the first five picoseconds of the pump-probe measurement in singly and doubly charged Hg_{17} . Even more surprising is our finding that cluster masses from the monomer up to at least $n = 43$ exhibit quite similar, if not identical, Fourier spectra in both singly and doubly charged species. We interpret the regular modulation of the ion intensity as demonstrating wave packet motion in a neutral cluster excited-state manifold. Fourier analysis reveals a very simple frequency spectrum of a group of low-frequency peaks around 26 cm^{-1} .

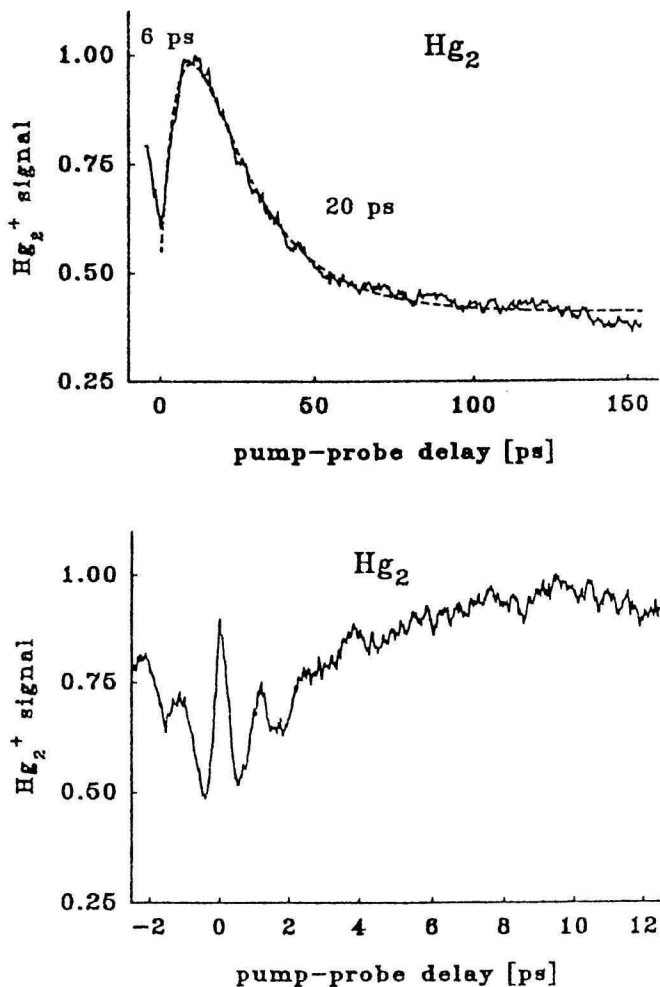


Fig. 11. Transient multiphoton ionization spectra of the mercury dimer obtained with 60 fs laser pulses at 620 nm.

The simplicity and similarity of the wave packet Fourier spectrum over a broad range of cluster masses lead us to propose multiphoton absorption to a core Hg_2^* 'chromophore' imbedded within and common to all the Hg_n neutral cluster examined in these experiments. The fact that blocking the probe pulse effectively quenches all ion signals and that the pump-probe spectrum with a weaker pump (or probe) is still symmetric with respect to $t=0$ means that the pump pulse must excite a manifold of high-lying Rydberg states near but below the individual cluster ionization limit. Wave packets associated with the Hg_2^* -core form and evolve within this manifold, and the variable-delay probe pulse

detects them by transferring the wave packet motion into both singly and doubly charged cluster ion channels. In addition to the simplicity and universality of the wave packet spectra, previous measurements of one-photon Hg_n -cluster absorption spectra by Brechignac et al. (29) support the idea of a common Hg_2^* chromophore. Their results show the persistence of autoionization features in the ionization spectra of mercury clusters up to $n \approx 35$.

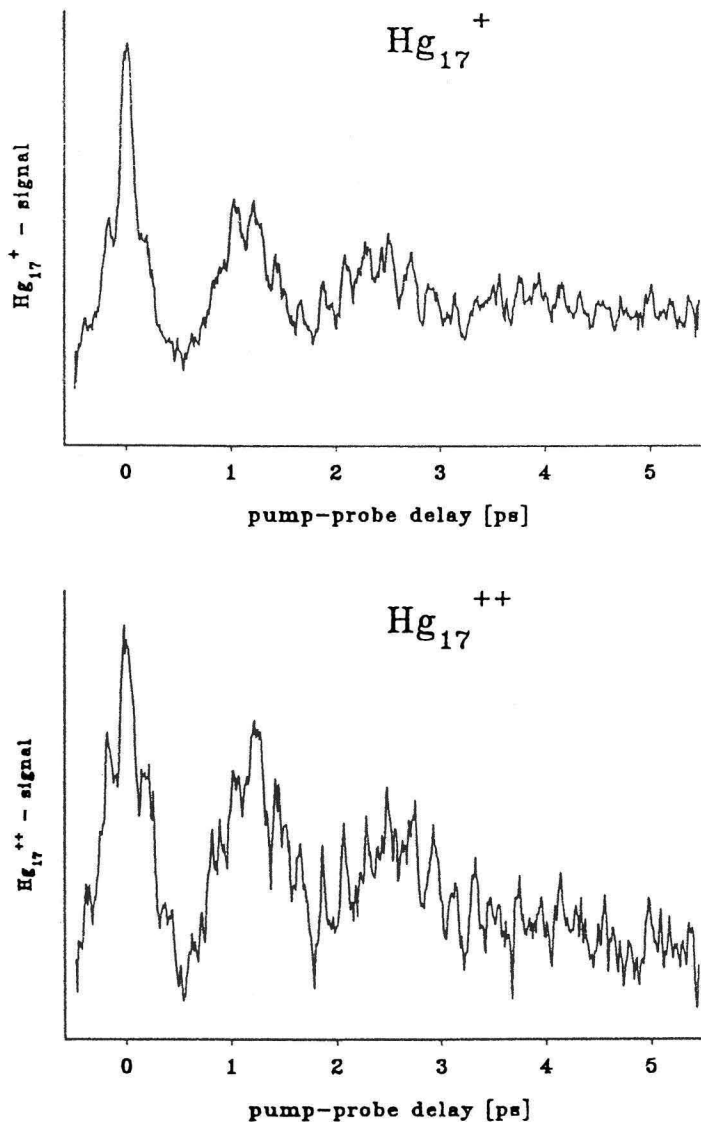


Fig. 12. Transient multiphoton ionization spectra of singly (upper part) and doubly (lower part) charged Hg_{17} cluster.

From the transient ionization spectra of singly and doubly charged Hg_{17} , shown in Fig. 12, it is clear that a maximum ion signal is observed for both species at precisely zero delay time. Note, this suggests that double ionization occurs directly through a transition from the neutral to the doubly charged manifold and not via the singly ionized continuum as it is observed in many high laser field experiments with atoms and molecules.

Summary

The real-time dynamics of multiphoton ionization and fragmentation of sodium and mercury molecules and cluster have been studied in beam experiments employing femtosecond pump-probe techniques and ion- and electron spectroscopy. Sodium with one valence electron per atom is an experimentally and theoretically very attractive system and metal prototype, whereas the divalent mercury offers the unique possibility to study the size dependent nonmetal-metal transition. Femtosecond time-resolved multi-photon ionization of sodium and mercury reveals unexpected features in the dynamics of the absorption of several photons like the observation of a second major REMPI process in Na_2 involving two electrons. Vibrational wave packet motions in dimers, trimers and even much larger systems like Na_8 and Na_{20} have been studied. The spreading and recurrence of a vibrational wave packet as well as its behaviour in strong laser fields have been studied in detail.

Cluster physics bridge the gap between molecular and solid state physics. Cluster size-dependent studies of physical properties such as absorption resonances, lifetimes and decay channels have been performed with tunable, ultrashort light pulses. A major result of our femtosecond experiments is that the conventional view of the optical response of metal-cluster, e.g. the absorption, ionization and decay processes as well as the corresponding time scales, had to be changed. Our results clearly show that for cluster sizes Na_n with $n \leq 21$, the molecular structure, excitations and properties prevail over collective excitations and surface-plasmon like properties. It is however obvious that for even larger cluster the optical response must finally be dominated by collective interactions. The preliminary analysis of the time-resolved mercury experiments gives astonishing results. First, the observation of singly and doubly ionized cluster in direct multiphoton ionization transitions and second, an almost identical vibrational wave packet motion in both singly and doubly charged cluster up to $n = 43$ is very surprising. Probably a Hg_2^* -chromophore imbedded within and common to all Hg_n neutral cluster carries the oscillator strength and determines the 'short' time wave packet dynamics.

These real-time studies of the dynamics of ionization and fragmentation with femtosecond time resolution open up new and very exciting fields in molecular and cluster physics and yield results which in many cases are not accessible in nanosecond or picosecond laser experiments.

We gratefully acknowledge the discussions with V. Engel and J. Weiner and the contributions of A. Assion, V. Gerstner, B. Lang, F. Sattler, V. Seyfried, C. Rothenfußer, C. Röttgermann and S. Vogler to various experiments. This work has been supported by the Deutsche Forschungsgemeinschaft through the Sonderforschungsbereich 276 in Freiburg.

References

1. Baumert, T., Bühler, B., Thalweiser, R., and Gerber, G., *Phys. Rev. Lett.* **64**, 733, 1990.
2. Keller, J., and Weiner, J., *Phys. Rev.* **A30**, 213, 1984; Burkhardt, C.E., Garver, W.P., and Leventhal, J.J., *Phys. Rev.* **A31**, 505, 1985.
3. Broyer, M., Delacretaz, G., Labastie, P., Whetten, R.L., Wolf, J.P., and Wöste, L., *Z. Phys.* **D 3**, 131, 1986.
4. Khundkar, L., and Zewail, A.H., *Annu. Rev. Phys. Chem.* **41**, 15, 1990, and references therein.
5. Ultrafast Phenomena VIII, eds. J.L. Martin, A. Migus, G.A. Mourou, and A.H. Zewail, Springer Series in Chemical Physics Vol. **55**, Springer Verlag, 1993.
6. Baumert, T., Grosser, M., Thalweiser, R., and Gerber, G., *Phys. Rev. Lett.* **67**, 3753, 1991.
7. Baumert, T., Bühler, B., Grosser, M., Thalweiser, R., Weiss, V., Wiedemann, E., and Gerber, G., *J. Phys. Chem.* **95**, 8103, 1991.
8. Engel, V., Baumert, T., Meier, Ch., and Gerber, G., *Z. Phys.* **D 28**, 37, 1993.
9. Baumert, T., Engel, V., Meier, C., and Gerber, G., *Chem. Phys. Lett.* **200**, 488, 1992.
10. Baumert, T., Engel, V., Röttgermann, C., Strunz, W.T., and Gerber, G., *Chem. Phys. Lett.* **191**, 639, 1992.
11. Baumert, T., Thalweiser, R., and Gerber, G., *Chem. Phys. Lett.* **209**, 29, 1993.
12. Delacretaz, G., Grant, E.R., Whetten, R.L., Wöste, L., and Zwanziger, J.F., *Phys. Rev. Lett.* **56**, 2598, 1986.
Rakowsky, S., Herrmann, F.W., and Ernst, W.E., *Z. Phys.* **D26**, 1993.
13. Broyer, M., Delacretaz, G., Ni, G.Q., Wetten, R.L., Wolf, J.P., and Wöste, L., *Phys. Rev. Lett.* **62**, 2100, 1989.
14. Meyer, W., priv. communication.
15. Cocchini, F., Upton, T.H., and Andreoni, W., *J. Chem. Phys.* **88**, 6068, 1988.
16. Meiswinkel, R., and Köppel, H., *Chem. Phys. Lett.* **144**, 177, 1990.
17. Baumert, T., Röttgermann, C., Rothenfußer, C., Thalweiser, R., Weiss, V., and Gerber, G., *Phys. Rev. Lett.* **69**, 1512, 1992.
18. Baumert, T., Thalweiser, R., Weiss, V., and Gerber, G., *Z. Phys.* **D 26**, 131 (1993).
19. Selby, K., Vollmer, M., Masui, J., Kresin, V., de Heer, W.A., and Knight, W.D., *Phys. Rev.* **B40**, 5417 (1989).

20. Wang, C.R., Pollak, S., Cameron, D., and Kappes, M.M., *J. Chem. Phys.* **93**, 3, 1990.
21. Kresin, V., *Physics Reports* **220**, 1 (1992)
22. Yannouleas, C., and Broglia, R.A., *Phys. Rev.* **A44**, 5793, 1991.
23. Ekardt, W., *Phys. Rev.* **B31**, 6360, 1985; Ekardt, W., Penzar, Z., *ibid.* **B43**, 1322, 1991.
24. Bonacic-Koutecky, V., Fantucci, P., and Koutecky, J., *Chem. Rev.* **91**, 1035, 1991 and *J. Chem. Phys.* **93**, 3802, 1990.
25. Rothenfußer, C., Thalweiser, R., Weiss, V., and Gerber, G., *Phys. Rev. Lett.* - submitted.
26. Thalweiser, R., Vogler, S., and Gerber, G., *SPIE Proceedings Vol.* **1858**, 196, 1993.
27. Rademann, K., Kaiser, B., Even, U., and Hensel, F., *Phys. Rev. Lett.* **59**, 2319, 1987.
28. Haberland, H., v. Issendorf, B., Yufeng, J., Kolar, T., and Thanner, G., *Z. Phys.* **D 26**, 8, 1993.
29. Brechignac, C., Broyer, M., Cahuzac, Ph., Delacretaz, G., Labastie, P., Wolf, J.P., and Wöste, L., *Phys. Rev. Lett.* **60**, 275, 1988.

Authors' Address:

Fakultät für Physik
Universität Freiburg
Herrmann-Herder-Str. 3
D-79104 Freiburg
Germany

